

## Article

# Antibladder Cancer Effects of Excavatolide C by Inducing Oxidative Stress, Apoptosis, and DNA Damage In Vitro

Che-Wei Yang<sup>1</sup>, Tsu-Ming Chien<sup>2,3,4</sup>, Chia-Hung Yen<sup>1</sup> , Wen-Jeng Wu<sup>2,3,4</sup>, Jyh-Horng Sheu<sup>5,6,\*</sup> and Hsueh-Wei Chang<sup>7,8,9,\*</sup> 

<sup>1</sup> Graduate Institute of Natural Products, Kaohsiung Medical University, Kaohsiung 80708, Taiwan; u110531013@gap.kmu.edu.tw (C.-W.Y.); chyen@kmu.edu.tw (C.-H.Y.)

<sup>2</sup> Graduate Institute of Clinical Medicine, College of Medicine, Kaohsiung Medical University, Kaohsiung 80756, Taiwan; u108801005@kmu.edu.tw (T.-M.C.); wejewu@kmu.edu.tw (W.-J.W.)

<sup>3</sup> Department of Urology, Kaohsiung Medical University Hospital, Kaohsiung 80756, Taiwan

<sup>4</sup> Department of Urology, Faculty of Medicine, College of Medicine, Kaohsiung Medical University, Kaohsiung 80756, Taiwan

<sup>5</sup> Department of Marine Biotechnology and Resources, National Sun Yat-sen University, Kaohsiung 80424, Taiwan

<sup>6</sup> Department of Medical Research, China Medical University Hospital, China Medical University, Taichung 40402, Taiwan

<sup>7</sup> Center for Cancer Research, Kaohsiung Medical University, Kaohsiung 80708, Taiwan

<sup>8</sup> Department of Medical Research, Kaohsiung Medical University Hospital, Kaohsiung Medical University, Kaohsiung 80708, Taiwan

<sup>9</sup> Department of Biomedical Science and Environmental Biology, College of Life Science, Kaohsiung Medical University, Kaohsiung 80708, Taiwan

\* Correspondence: sheu@mail.nsysu.edu.tw (J.-H.S.); changhw@kmu.edu.tw (H.-W.C.); Tel.: +886-7-525-2000 (ext. 5030) (J.-H.S.); +886-7-312-1101 (ext. 2691) (H.-W.C.)



**Citation:** Yang, C.-W.; Chien, T.-M.;

Yen, C.-H.; Wu, W.-J.; Sheu, J.-H.;

Chang, H.-W. Antibladder Cancer Effects of Excavatolide C by Inducing Oxidative Stress, Apoptosis, and DNA Damage In Vitro. *Pharmaceuticals* **2022**, *15*, 917.

[https://doi.org/10.3390/](https://doi.org/10.3390/ph15080917)

[ph15080917](https://doi.org/10.3390/ph15080917)

Academic Editors:

Marianna Carbone and Maria

Letizia Ciavatta

Received: 19 June 2022

Accepted: 21 July 2022

Published: 24 July 2022

**Publisher's Note:** MDPI stays neutral with regard to jurisdictional claims in published maps and institutional affiliations.



**Copyright:** © 2022 by the authors. Licensee MDPI, Basel, Switzerland. This article is an open access article distributed under the terms and conditions of the Creative Commons Attribution (CC BY) license (<https://creativecommons.org/licenses/by/4.0/>).

**Abstract:** Excavatolide C (EXCC) is a bioactive compound derived from the gorgonian octocoral *Briareum excavatum*, and its anticancer effects are rarely addressed, particularly for bladder cancer. This investigation aimed to explore the potential impacts of EXCC on inhibiting the proliferation of three kinds of bladder cancer cells (5637, BFTC905, and T24). EXCC inhibits bladder cancer cell proliferation based on 48 h ATP assay. This antiproliferation function is validated to be oxidative stress dependent. Cellular and mitochondrial oxidative stresses were upregulated by EXCC, accompanied by depleting glutathione and mitochondrial membrane potential. These antiproliferation and oxidative stress events were suppressed by *N*-acetylcysteine (NAC), indicating that EXCC has an oxidative stress-regulating function for antiproliferation of bladder cancer cells. Oxidative stress-related responses such as apoptosis, caspase activation, and DNA damage were upregulated by EXCC and reverted by NAC. Taken together, the antiproliferation function of EXCC provides a potential treatment against bladder cancer cells via oxidative stress modulation.

**Keywords:** soft coral; bladder cancer; apoptosis; oxidative stress; DNA damage

## 1. Introduction

Bladder cancer was the eighth leading cause of cancer death according to the United States Cancer Statistics [1]. Its estimated new cases and deaths for both genders were 83,730 and 17,200 for bladder cancer patients [1]. Bladder tumors are commonly treated by radical cystectomy coupled with cisplatin-based chemotherapy [2,3]. However, cisplatin occasionally generates adverse effects [4,5]. Therefore, it is critical to identify more antiproliferation agents for bladder cancer treatment.

Marine corals containing different natural products [6,7] were reported for anticancer treatment [8–11]. The gorgonian soft coral *Briareum excavatum* (*B. excavatum*) is commonly screened for natural products. Several bioactive compounds were reported from *B. excavatum* [12–18], and some studies provide their chemical characterizations. In some

studies, the antiproliferation effects against several cancer cells were investigated. However, they generally offered cytotoxicity with  $IC_{50}$  values and lacked investigations of detailed anticancer mechanisms.

The  $\alpha,\beta$ -epoxy- $\gamma$ -lactone motif commonly existed in several natural products with anticancer effects, such as lophotoxin [19] and bipinnatin Q [20], for antileukemia function. Several *B. excavatum*-derived excavatolide compounds, such as excavatolide B-E, contain this  $\alpha,\beta$ -epoxy- $\gamma$ -lactone motif. Excavatolide B is the most abundant *B. excavatum*-derived metabolite providing the generation of oxidative stress and antiproliferation in lung cancer cells [21]. However, the anticancer study for another excavatolide, namely excavatolide C (EXCC), was rarely investigated. EXCC was discovered in 1998 [12] and showed cytotoxicity ( $IC_{50}$  values) to lung and colon cancer cells. However, the anticancer mechanisms of EXCC remain unclear.

This investigation aims to evaluate the antiproliferation impacts of EXCC against bladder cancer cells. Anticancer mechanisms of oxidative stress were the particular objective, as well as associated changes, such as apoptosis and DNA damage to bladder cancer cells.

## 2. Results

### 2.1. Proliferation Change by EXCC

The modulating impacts of proliferation of EXCC (Figure 1A) were tested using three kinds of bladder cancer cell lines (5637, BFTC905, and T24). EXCC at 48 h treatment dose-responsively reduced the cell viability of these bladder cancer cells (Figure 1B). To assess the effects of oxidative stress, an inhibitor of oxidative stress such as *N*-acetylcysteine (NAC) was pretreated before EXCC treatment, i.e., NAC/EXCC. Subsequently, antiproliferation effects exerted by EXCC were suppressed by NAC (NAC/EXCC), and their cell viabilities were recovered to similar levels as in the control (Figure 1C).

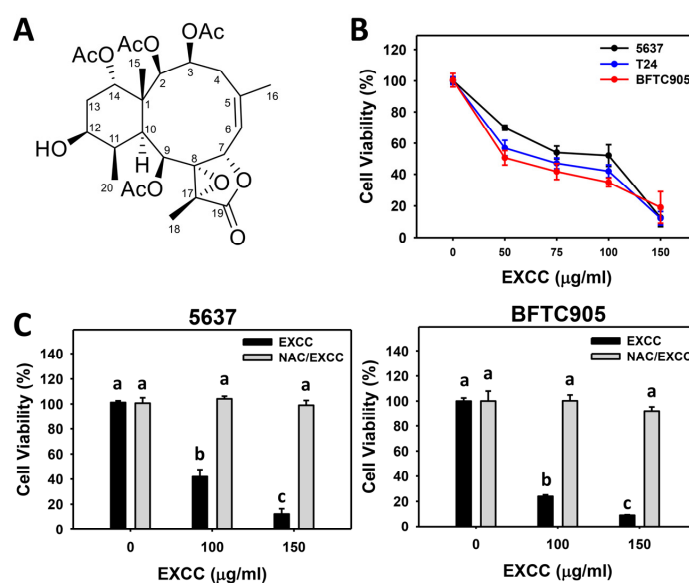


**Figure 1.** Proliferation change by EXCC. (A) Structure. (B) ATP assay of EXCC. Three bladder cancer cell lines (5637, BFTC905, and T24) were tested. Cells were treated with control (0.1% DMSO) and EXCC for 48 h and subjected to an ATP assay to determine cell viability. (C) ATP assay of NAC/EXCC. *N*-acetylcysteine (NAC)/EXCC is the NAC pretreatment (10 mM, 1 h) coupled with EXCC posttreatment (100 and 150  $\mu\text{g}/\text{mL}$ , 48 h). Statistical lower-case letters were given to each treatment. Non-overlapping letters between different treatments indicate significant results ( $p < 0.05$ ). Data, means  $\pm$  SD ( $n = 3$ ). For example (5637 cells in Figure 1C), the EXCC (black color) 0, 100, and 150 indicating “a, b, and c” show significant results between each other because these letters were non-overlapping. In contrast, EXCC 0 (black color) and NAC/EXCC (gray color) 0, 100, and 150 indicating “a” show nonsignificant results because these letters overlap.

## 2.2. Cell Cycle Change by EXCC

EXCC at 48 h treatment upregulated the subG1 (%) of bladder cancer cells (5637 and BTFC905) (Figure 2). To evaluate the effect of oxidative stress in the cell cycle progression, NAC was pretreated before EXCC treatment. Subsequently, the subG1 increment exerted by EXCC was suppressed by NAC (NAC/EXCC), and their subG1 (%) was recovered similar to the control (Figure 2).

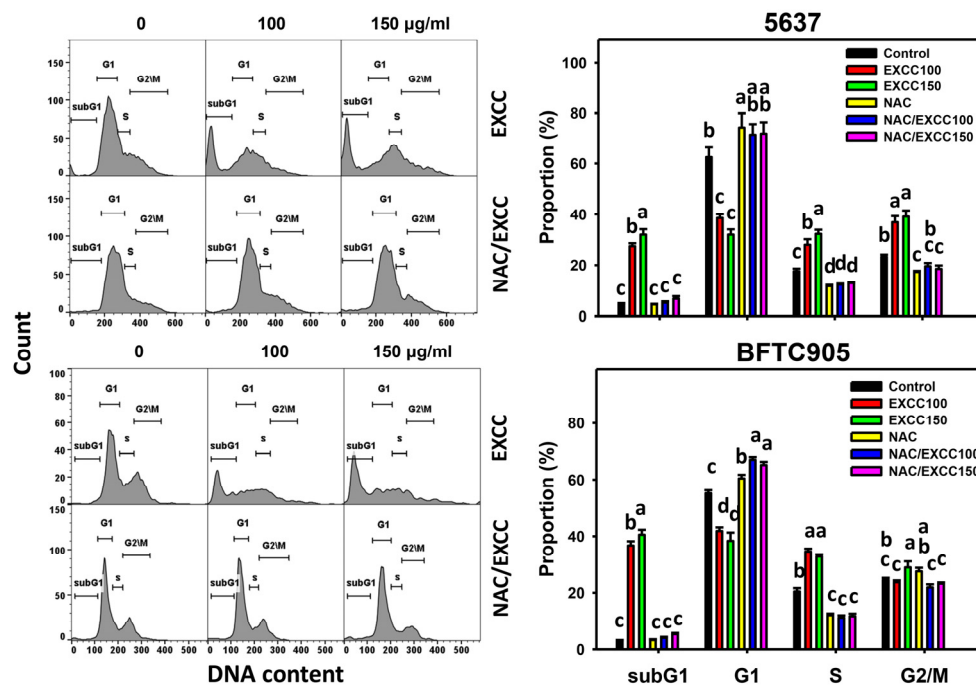


**Figure 2.** Cell cycle change by EXCC and NAC/EXCC. Two bladder cancer cell lines (5637 and BTFC905) were tested. Cells were treated with control (0.1% DMSO) and EXCC (100 and 150 µg/mL) for 48 h. NAC/EXCC is the NAC pretreatment (10 mM, 1 h) coupled with EXCC posttreatment (100 and 150 µg/mL, 48 h). Statistically different lower-case letters were given to each treatment. Non-overlapping letters between different treatments indicate significant results ( $p < 0.05$ ). Data, means  $\pm$  SD ( $n = 3$ ). For the example of subG1 (5637 cells), the EXCC 0 (control), 100, and 150 indicating “c, b and a” show significant results between each other because these letters were non-overlapping. In contrast, NAC, NAC/EXCC 100, and NAC/EXCC 150 indicating “c” show nonsignificant results because these letters overlap.

In addition to subG1 changes, EXCC affected other cell phases in bladder cancer cells. For 5637 bladder cancer cells, EXCC decreased the G1 phase and increased S and G2/M phases, which were reverted by NAC (Figure 2). For BTFC905 cells, EXCC decreased G1 and increased S phases, which NAC reverted.

## 2.3. Apoptosis (Annexin V) Change by EXCC

Annexin V detection is one of the apoptosis indicators [22]. EXCC at 48 h treatment upregulated the annexin V (+) (%) of bladder cancer cells (5637 and BTFC905) (Figure 3A). To assess the participation of oxidative stress in apoptosis, NAC was pretreated before EXCC treatment. Subsequently, the annexin V (+) increment exerted by EXCC was suppressed by NAC (NAC/EXCC), and their annexin V (+) (%) was recovered similar to the control (Figure 3B).

## 2.4. Caspase 3 (Cas 3) Activation Change by EXCC

Cas 3 activation is one of the apoptosis indicators [23]. EXCC at 48 h treatment upregulated the Cas 3 (+) (%) of bladder cancer cells (5637 and BTFC905) (Figure 4A). To assess the participation of oxidative stress in apoptosis, NAC was pretreated before EXCC

treatment. Subsequently, the Cas 3 (+) increment exerted by EXCC was suppressed by NAC (NAC/EXCC), and their Cas 3 (+) (%) was recovered like control (Figure 4B).

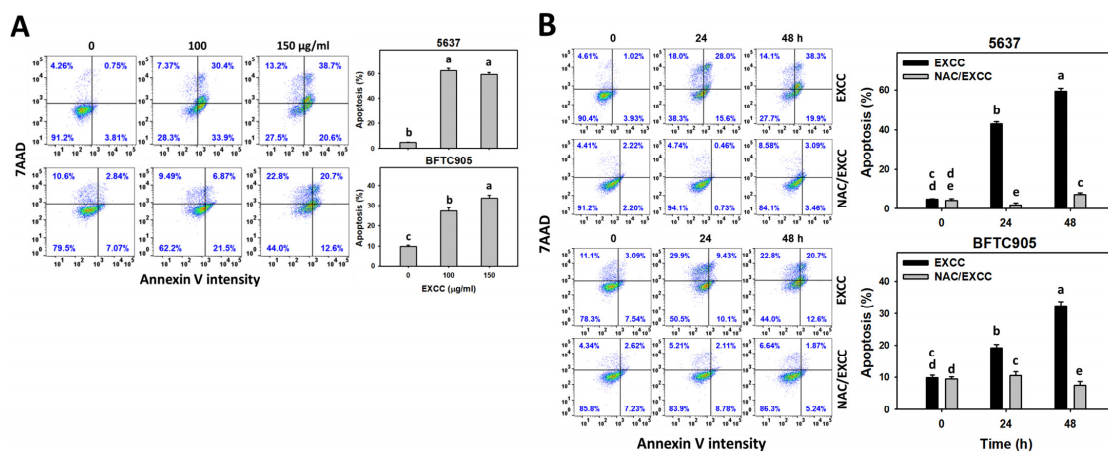


**Figure 3.** Apoptosis (annexin V) change by EXCC. (A) Annexin V assay of EXCC. Two bladder cancer cell lines (5637 and BFTC905) were tested. Cells were treated with control (0.1% DMSO) and EXCC (100 and 150 µg/mL) for 48 h. Apoptosis (%) was determined by calculation of annexin V (+)/7AAD (±) (%). (B) Annexin V assay of NAC/EXCC. NAC/EXCC was NAC pretreatment (10 mM, 1 h) coupled with EXCC posttreatment (100 and 150 µg/mL, 24 and 48 h). Statistical lower-case letters were given to each treatment. Non-overlapping letters between different treatments indicate significant results ( $p < 0.05$ ). Data, means  $\pm$  SD ( $n = 3$ ). For example (5637 cells in Figure 3B), the EXCC (black color) 0, 24, and 48 h indicating “cd, b and a” show significant results between each other because these letters were not overlapping. In contrast, EXCC 0 (black color) and NAC/EXCC (gray color) 0 h indicating “cd and de” show nonsignificant results because these letters were overlapping with “d”.

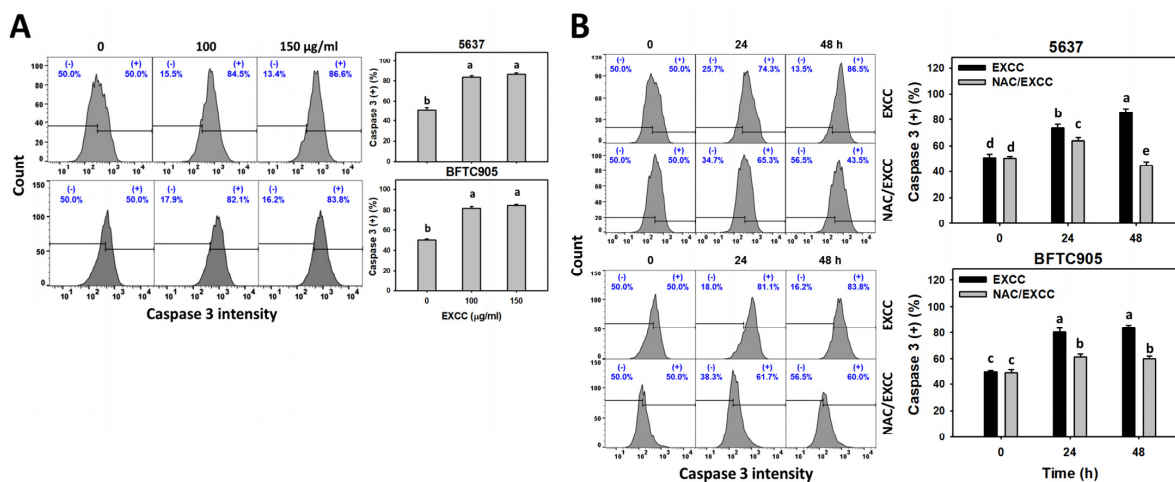


**Figure 4.** Cas 3 activation change by EXCC. (A) Cas 3 assays of EXCC. Two bladder cancer cell lines (5637 and BFTC905) were tested. Cells were treated with control (0.1% DMSO) and EXCC (100 and 150 µg/mL) for 48 h. (+) represents the Cas 3 (+) population. (B) Cas 3 assays of NAC/EXCC. NAC/EXCC is the NAC pretreatment (10 mM, 1 h) coupled with EXCC posttreatment (150 µg/mL, 24 and 48 h). Statistical lower-case letters were given to each treatment. Non-overlapping letters between different treatments indicate significant results ( $p < 0.05$ ). Data, means  $\pm$  SD ( $n = 3$ ). For example (5637 cells in Figure 4B), the EXCC (black color) 0, 24, and 48 h indicating “d, b, and a” show significant results between each other because these letters were non-overlapping. In contrast, EXCC 0 (black color) and NAC/EXCC (gray color) 0 h indicating “d” show nonsignificant results because these letters overlap.

### 2.5. Caspase 8/9 (Cas 8/9) Changes by EXCC

Cas 8/9 activations are extrinsic and intrinsic apoptosis indicators [23]. EXCC at 48 h treatment upregulated the Cas 8/9 (+) (%) of bladder cancer cells (5637 and BTFC905) (Figure 5A,C). To evaluate the participation of oxidative stress in apoptosis, NAC was pretreated before EXCC treatment. Subsequently, the Cas 8/9 (+) (%) increment exerted by EXCC was suppressed by NAC (NAC/EXCC), and their Cas 8/9 (+) (%) was recovered like control (Figure 5B,D).

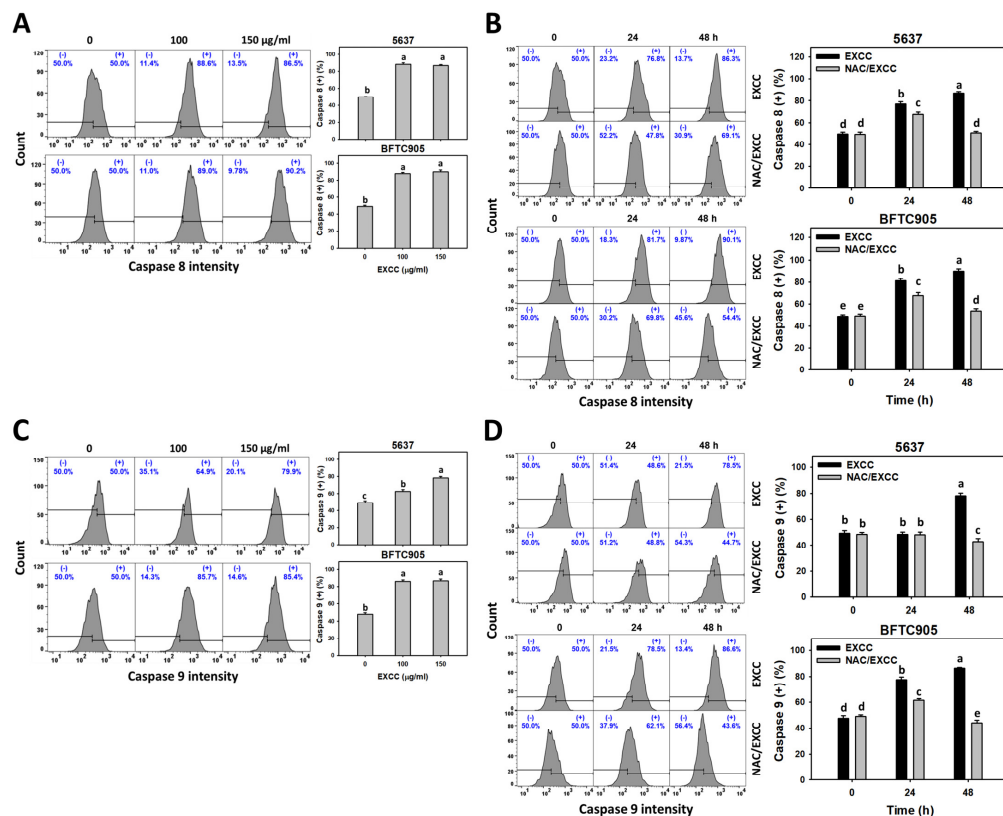


**Figure 5.** Cas 8 and Cas 9 changes by EXCC. (A,C) Cas 8 and Cas 9 assays of EXCC. Two bladder cancer cell lines (5637 and BTFC905) were tested. Cells were treated with control (0.1% DMSO) and EXCC (100 and 150 µg/mL) for 48 h. (+) represents the Cas 8 or Cas 9 (+) population. (B,D) Cas 8 and Cas 9 assays of NAC/EXCC. NAC/EXCC is the NAC pretreatment (10 mM, 1 h) coupled with EXCC posttreatment (150 µg/mL, 24 and 48 h). Statistical lower-case letters were given to each treatment. Non-overlapping letters between different treatments indicate significant results ( $p < 0.05$ ). Data, means  $\pm$  SD ( $n = 3$ ). For example (5637 cells in Figure 5B), the EXCC (black color) 0, 24, and 48 h indicating “d, b and a” show significant results between each other because these letters were non-overlapping. In contrast, EXCC 0 (black color) and NAC/EXCC (gray color) 0 h indicating “d” show nonsignificant results because these letters overlap.

### 2.6. Oxidative Stress Change by EXCC

The depletion effects of oxidative stress were tested with NAC (Figures 1–5). However, the oxidative stress changes were not examined for EXCC treatment in bladder cancer cells. Using the specific probes for reactive oxygen species (ROS) and mitochondrial superoxide (MitoSOX) [24], different kinds of oxidative stresses were monitored.

EXCC at 9 and 48 h treatments upregulated the ROS and MitoSOX (+) (%) of bladder cancer cells (5637 and BTFC905) (Figures 6A and 7A). To evaluate the participation of oxidative stress, NAC was pretreated before EXCC treatment. Subsequently, the ROS and MitoSOX (+) (%) increment exerted by EXCC was suppressed by NAC (NAC/EXCC), and their ROS and MitoSOX (+) (%) was recovered similar to the control (Figures 6B and 7B).

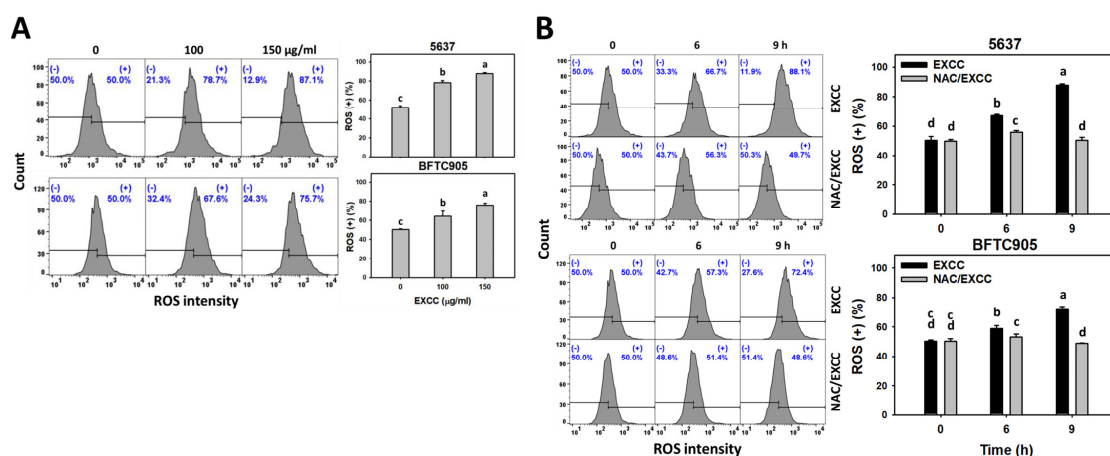


**Figure 6.** ROS change by EXCC. (A) ROS assay of EXCC. Two bladder cancer cell lines (5637 and BFTC905) were tested. Cells were treated with control (0.1% DMSO) and EXCC (100 and 150 µg/mL) for 9 h. (+) represents ROS (+) population. (B) ROS assay of NAC/EXCC. NAC/EXCC is the NAC pretreatment (10 mM, 1 h) coupled with EXCC posttreatment (150 µg/mL, 6 and 9 h). Statistical lower-case letters were given to each treatment. Non-overlapping letters between different treatments indicate significant results ( $p < 0.05$ ). Data, means  $\pm$  SD ( $n = 3$ ). For example (5637 cells in Figure 6B), the EXCC (black color) 0, 6, and 9 h indicating “d, b, and a” show significant results between each other because these letters were non-overlapping. In contrast, EXCC 0 (black color) and NAC/EXCC (gray color) 0 h indicating “d” show nonsignificant results because these letters overlap.

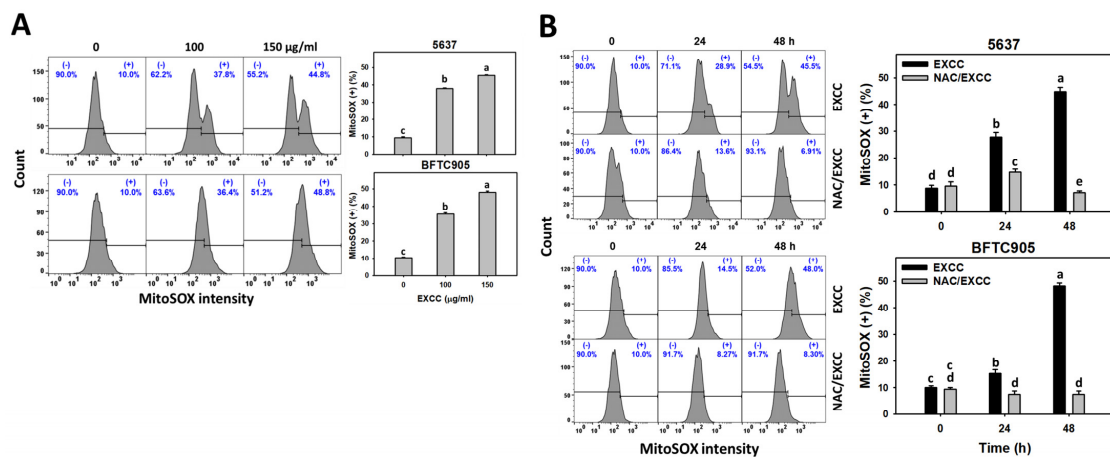


**Figure 7.** MitoSOX change by EXCC. (A) MitoSOX assay of EXCC. Two bladder cancer cell lines (5637 and BFTC905) were tested. Cells were treated with control (0.1% DMSO) and EXCC (100 and 150 µg/mL) for 48 h. (+) represents MitoSOX (+) population. (B) MitoSOX assay of NAC/EXCC. NAC/EXCC is the NAC pretreatment (10 mM, 1 h) coupled with EXCC posttreatment (150 µg/mL, 24 and 48 h). Statistical lower-case letters were given to each treatment. Non-overlapping letters between different treatments indicate significant results ( $p < 0.05$ ). Data, means  $\pm$  SD ( $n = 3$ ). For example (5637 cells in Figure 7B), the EXCC (black color) 0, 24, and 48 h indicating “d, b, and a” show significant results between each other because these letters were non-overlapping. In contrast, EXCC 0 (black color) and NAC/EXCC (gray color) 0 h indicating “d” show nonsignificant results because these letters overlap.

EXCC at 48 h treatment upregulated the glutathione (GSH) (–) (%) of bladder cancer cells (5637 and BFTC905) (Figure 8A). To evaluate the participation of oxidative stress, NAC was pretreated before EXCC treatment. Subsequently, the GSH (–) (%) increment exerted by EXCC was suppressed by NAC (NAC/EXCC), and their GSH (–) (%) was recovered similar to the control (Figure 8B).

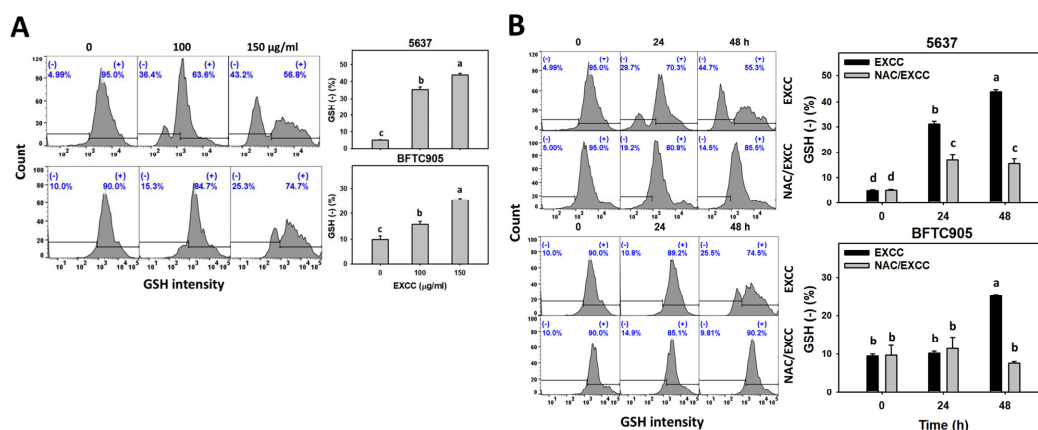


**Figure 8.** GSH change by EXCC. **(A)** GSH assay of EXCC. Two bladder cancer cell lines (5637 and BFTC905) were tested. Cells were treated with control (0.1% DMSO) and EXCC (100 and 150 µg/mL) for 48 h. (–) represents GSH (–) population. **(B)** GSH assay of NAC/EXCC. NAC/EXCC is the NAC pretreatment (10 mM, 1 h) coupled with EXCC posttreatment (150 µg/mL, 24 and 48 h). Statistical lower-case letters were given to each treatment. Non-overlapping letters between different treatments indicate significant results ( $p < 0.05$ ). Data, means  $\pm$  SD ( $n = 3$ ). For example (5637 cells in Figure 8B), the EXCC (black color) 0, 24, and 48 h indicating “d, b, and a” show significant results between each other because these letters were non-overlapping. In contrast, EXCC 0 (black color) and NAC/EXCC (gray color) 0 h indicating “d” show nonsignificant results because these letters overlap.

### 2.7. Mitochondrial Membrane Potential (MMP) Change by EXCC

MMP is another indicator for evaluating oxidative stress [25,26]. EXCC at 48 h treatment upregulated the MMP (–) (%) of bladder cancer cells (5637 and BFTC905) (Figure 9A). To evaluate the participation of oxidative stress, NAC was applied before EXCC treatment. Subsequently, the MMP (–) (%) increment exerted by EXCC was suppressed by NAC (NAC/EXCC), and their MMP (–) (%) was recovered similar to the control (Figure 9B).

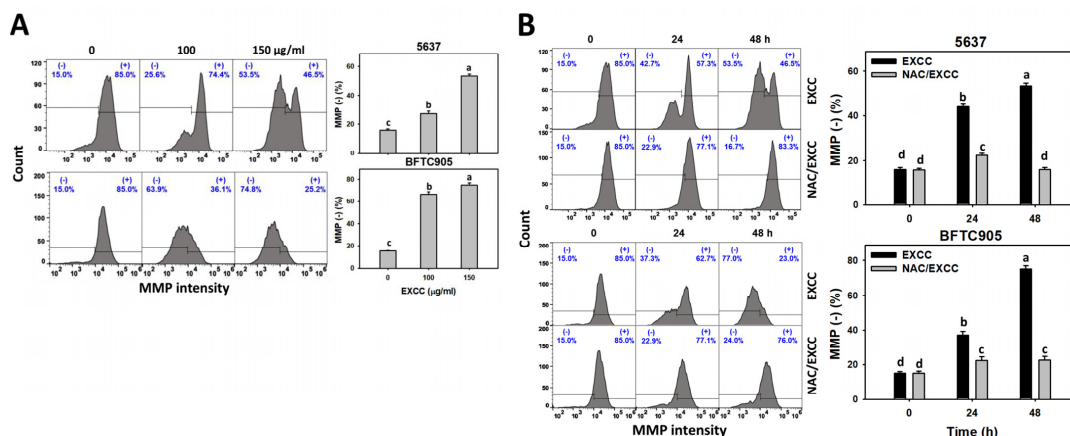


**Figure 9.** MMP change by EXCC. **(A)** MMP assay of EXCC. Two bladder cancer cell lines (5637 and BFTC905) were tested. Cells were treated with control (0.1% DMSO) and EXCC (100 and 150 µg/mL) for 48 h. (–) represents MMP (–) population. **(B)** MMP assay of NAC/EXCC. NAC/EXCC is the NAC pretreatment (10 mM, 1 h) coupled with EXCC posttreatment (150 µg/mL, 24 and 48 h). Statistical lower-case letters were given to each treatment. Non-overlapping letters between different treatments indicate significant results ( $p < 0.05$ ). Data, means  $\pm$  SD ( $n = 3$ ). For example (5637 cells in Figure 9B), the EXCC (black color) 0, 24, and 48 h indicating “d, b, and a” show significant results between each other because these letters were non-overlapping. In contrast, EXCC 0 (black color) and NAC/EXCC (gray color) 0 h indicating “d” show nonsignificant results because these letters overlap.

## 2.8. DNA Damage Change by EXCC

EXCC at 48 h treatment upregulated the  $\gamma$ H2AX and 8-hydroxy-2'-deoxyguanosine (8-OHdG) (+) (%) of bladder cancer cells (5637 and BTFC905) (Figures 10A and 11A). To evaluate the participation of oxidative stress, NAC was pretreated before EXCC treatment. Subsequently, the  $\gamma$ H2AX and 8-OHdG (+) (%) increment exerted by EXCC was suppressed by NAC (NAC/EXCC), and their  $\gamma$ H2AX and 8-OHdG (+) (%) was recovered similar to the control (Figures 10B and 11B).

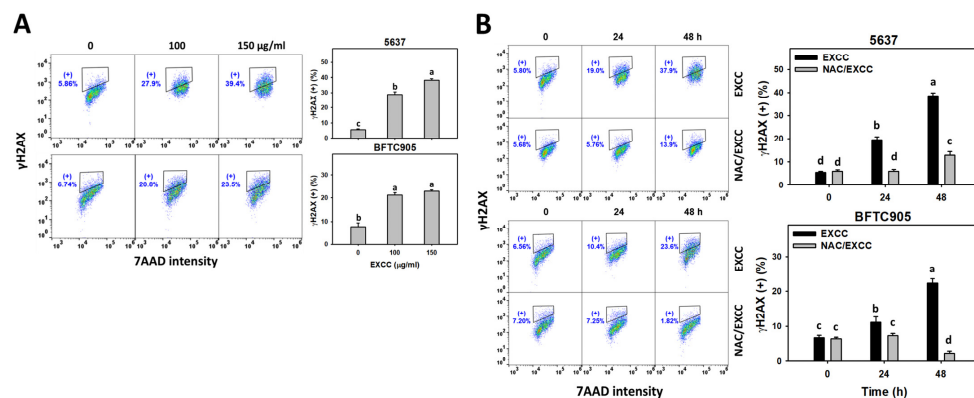


**Figure 10.**  $\gamma$ H2AX change by EXCC. (A)  $\gamma$ H2AX assay of EXCC. Two bladder cancer cell lines (5637 and BTFC905) were tested. Cells were treated with solvent control (0.1% DMSO) and EXCC (100 and 150  $\mu$ g/mL) for 48 h. (+) represents the  $\gamma$ H2AX (+) population. (B)  $\gamma$ H2AX assay of NAC/EXCC. NAC/EXCC is the NAC pretreatment (10 mM, 1 h) coupled with EXCC posttreatment (150  $\mu$ g/mL, 24 and 48 h). Statistical lower-case letters were given to each treatment. Non-overlapping letters between different treatments indicate significant results ( $p < 0.05$ ). Data, means  $\pm$  SD ( $n = 3$ ). For example (5637 cells in Figure 10B), the EXCC (black color) 0, 24, and 48 h indicating “d, b, and a” show significant results between each other because these letters were non-overlapping. In contrast, EXCC 0 (black color) and NAC/EXCC (gray color) 0 h indicating “d” show nonsignificant results because these letters overlap.

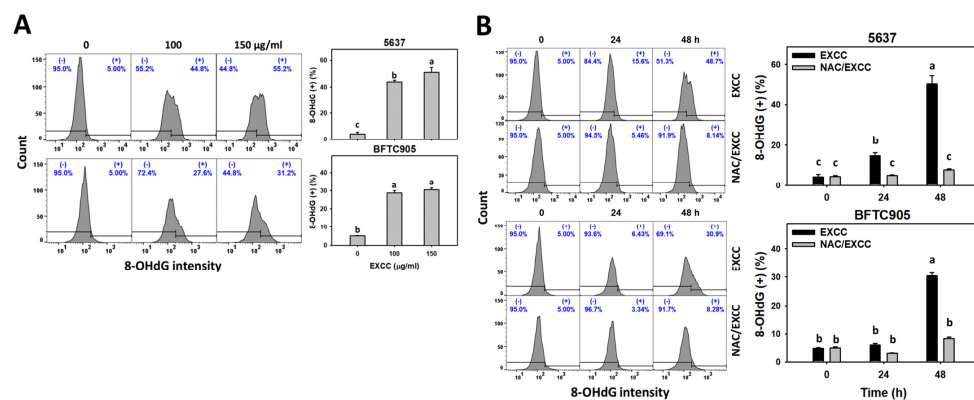


**Figure 11.** 8-OHdG change by EXCC. (A) 8-OHdG assay of EXCC. Two bladder cancer cell lines (5637 and BTFC905) were tested. Cells were treated with control (0.1% DMSO) and EXCC (100 and 150  $\mu$ g/mL) for 48 h. (+) represents the 8-OHdG (+) population. (B) 8-OHdG assay of NAC/EXCC. NAC/EXCC is the NAC pretreatment (10 mM, 1 h) coupled with EXCC posttreatment (150  $\mu$ g/mL, 24 and 48 h). Statistical lower-case letters were given to each treatment. Non-overlapping letters between different treatments indicate significant results ( $p < 0.05$ ). Data, means  $\pm$  SD ( $n = 3$ ). For example (5637 cells in Figure 11B), the EXCC (black color) 0, 24, and 48 h indicating “c, b, and a” show significant results between each other because these letters were non-overlapping. In contrast, EXCC 0 (black color) and NAC/EXCC (gray color) 0 h indicating “c” show nonsignificant results because these letters overlap.



### 3. Discussion

*B. excavatum*-derived EXCC showed cytotoxicity to lung and colon cancer cells. However, the anticancer mechanisms of EXCC remain unclear. The present study validates this hypothesis and confirms that EXCC induces apoptosis and DNA damage to bladder cancer cells.

#### 3.1. Comparison of Antiproliferation of EXCC in Different Cancer Cell Lines

The IC<sub>50</sub> value of EXCC for lung (A549) and colon (HT-29) cancer cells were 1.9 µg/mL, according to 72 h MTT assays [12]. In the present study, the IC<sub>50</sub> values of EXCC for bladder (BFTC905, T24, and 5637) cancer cells were 51, 62, and 100 µg/mL according to a 48 h ATP assay (Figure 1). Accordingly, EXCC showed different drug sensitivities to various cancer cells.

For comparison, cisplatin, a common clinical drug for bladder cancer, showed IC<sub>50</sub> values of 1.33 and 4.98 µg/mL for T24 and J82 cells at 48 h CCK-8 assay, respectively [27]. Cisplatin also showed IC<sub>50</sub> values of 4.79, 8.61, 38.54, and 27.85 µg/mL for 5637, J82, HT119, and 253J cells at 96 h trypan blue assay, respectively [28]. Notably, cisplatin showed severe side effects in clinical use [29]. It warrants a detailed assessment of the cytotoxicity of a non-cancer cell line to evaluate the selectivity of EXCC in the future.

#### 3.2. Role of Oxidative Stress in Antiproliferation of EXCC

Oxidative stress-generating drugs commonly inhibit cancer cell proliferation [30–33]. For example, cryptocaryone triggers ROS and apoptosis to inhibit the proliferation of ovarian cancer cells [34]. A marine natural product such as fucoidan can upregulate oxidative stress and consequently induce apoptosis and cause antiproliferation of oral cancer cells [33]. Excavatolide B induces ROS and RNS production, leading to antiproliferation in lung cancer cells [21]. After examination, EXCC caused antiproliferation, cellular and mitochondrial oxidative stress such as ROS and MitoSOX, and MMP depletion in bladder cancer cells (Figures 6, 7 and 9). These antiproliferation (Figure 1C) and oxidative stresses were suppressed by NAC, suggesting that EXCC exerts an oxidative stress-mediated antiproliferation to bladder cancer cells.

Moreover, redox homeostasis is balanced by oxidants and antioxidants [35,36]. GSH is one of the cellular antioxidants that downregulates oxidative stress [37,38]. Accordingly, GSH depletion leads to increased oxidative stress [31]. For example, fucoidan shows oxidative stress in oral cancer cells accompanied by GSH depletion. EXCC demonstrates a similar result in bladder cancer cells (Figure 8). Accordingly, EXCC downregulates GSH to trigger oxidative stress in bladder cancer cells.

#### 3.3. Apoptosis and DNA Damage Effects of EXCC Involving Oxidative Stress

Oxidative stress may evoke several cellular responses, such as apoptosis [39] and DNA damage [31]. For example, cryptocaryone-induced ROS promotes apoptosis and DNA damage in ovarian cancer cells [34]. Similarly, EXCC triggers apoptosis as evidenced by the cell cycle, annexin V, and caspase signaling (Figures 2–4). The present study showed that EXCC increases subG1 events of bladder cancer cells (Figure 2), which is the apoptosis-like changes. This is further validated by annexin V detection (Figure 3). Consistently, EXCC also activates apoptosis executor caspase 3 (Figure 4). Moreover, EXCC triggered both extrinsic and intrinsic caspase activations such as caspases 8 and 9 in bladder cancer cells (Figure 5). These apoptosis changes and signaling activations were suppressed by NAC, suggesting that EXCC triggers oxidative stress-mediated apoptosis in bladder cancer cells.

In addition, EXCC promotes DNA damage as evidenced by upregulating γH2AX and 8-OHdG expressions for DNA double-strand breaks and oxidative DNA damage in bladder cancer cells (Figures 10 and 11), which were suppressed by NAC, suggesting that EXCC exerts oxidative stress-mediated DNA damage to bladder cancer cells.

## 4. Materials and Methods

### 4.1. Extraction and Separation of EXCC

The gorgonian *B. excavatum* was harvested, freeze-dried, and minced as detailed in our previous study [12]. Then, the materials were extracted repeatedly by ethyl acetate (EtOAc). The combined organic extract was processed for evaporation and a dark green residue was generated. This was dissolved in EtOAc and then stored at 0 °C to provide a solid, representing a mixture of long-chained esters. After discarding this solid, the remaining mixture was purified by Si gel column chromatography, using hexane and hexane-EtOAc mixtures of increasing polarity. EXCC was obtained from a fraction eluted with hexane-EtOAc (3:1–2:1), which was further confirmed to be pure by melting point analyses (134–135 °C) and data from NMR spectroscopy (Supplementary Figures S1–S7).

### 4.2. Oxidative Stress Inhibitor

Pretreatment with NAC (10 mM, 1 h) (Sigma-Aldrich, St. Louis, MO, USA) [40–42] was applied to inhibit oxidative stress to examine its role in EXCC-induced changes.

### 4.3. Cell Culture and Viability

Three human bladder cancer cell lines were purchased from ATCC (Manassas, VA, USA) and Bioresource Collection and Research Center (BCRC) (Hsinchu, Taiwan), i.e., ATCC: 5637, T24, and BCRC: BFTC905. The culture medium was obtained from Roswell Park Memorial Institute (RPMI) medium (Gibco, Grand Island, NY, USA), containing 10% fetal bovine serum (FBS), 100 U/mL penicillin, and 100 µg/mL streptomycin. Cell viability was estimated by an ATP kit (PerkinElmer Life Sciences, Boston, MA, USA) following the user manual's instructions.

### 4.4. Cell Cycle Assays

Following fixation with 75% ethanol, cells were stained by 7-aminoactinomycin D (Biotium, Inc., Hayward, CA, USA) (7AAD; 1 µg/mL, 30 min) [43] and analyzed by Guava easyCyte flow cytometry (Luminex, Austin, TX, USA). The cell cycle phases were determined by their different DNA contents.

### 4.5. Apoptosis (Annexin V/7AAD)

Annexin V/7AAD reagents (Strong Biotech Inc., Taipei, Taiwan), containing Annexin V-FITC and 7AAD at the final condition (1:1000 and 1 µg/mL), were incubated with cells for 30 min to detect apoptosis [33,44] according to the user's manual. Finally, cells were analyzed by flow cytometry.

### 4.6. Apoptosis (Cas 3, 8, 9)

In addition to the apoptosis executor Cas 3, the extrinsic and intrinsic apoptosis caspases (Cas 8 and Cas 9) were assessed by OncoImmunin kits (Gaithersburg, MD, USA) [45,46]. PhiPhiLux-G1D2, CaspaLux8-L1D2, and CaspaLux9-M1D2, the specific substrates for Cas 3, Cas 8, and Cas 9, were mixed with cell suspensions (1:1000) at 37 °C for 1 h. The activated forms of Cas 3, Cas 8, and Cas 9 can cleave these substrates to generate green fluorescence, analyzed by flow cytometry.

### 4.7. ROS, MitoSOX, and GSH

ROS, MitoSOX, and GSH detecting reagents such as 2',7'-dichlorodihydrofluorescein diacetate (DCFH-DA) [33,47], MitoSOX™ Red [48], and 5-chloromethylfluorescein diacetate (CMF-DA) [49] were utilized to monitor oxidative stress. They were purchased commercially, i.e., Molecular Probes, Invitrogen, Eugene, OR, USA; Sigma-Aldrich, St. Louis, MO, USA; and Thermo Fisher Scientific, Carlsbad, CA, USA, respectively. The final conditions for DCFH-DA, MitoSOX™ Red, and CMF-DA were 2, 5, and 5 µM for 30 min, respectively. Finally, the cells were analyzed by flow cytometry.

#### 4.8. MMP

MMP detecting reagents, such as DiOC<sub>2</sub> (3), were utilized to monitor oxidative stress [33]. It was purchased from Invitrogen (San Diego, CA, USA). The final condition for DiOC<sub>2</sub> (3) was 50 nM for 20 min. Finally, the cells were analyzed by flow cytometry.

#### 4.9. $\gamma$ H2AX

After fixation, the  $\gamma$ H2AX-detecting antibody was utilized to monitor DNA double-strand breaks [33]. It was purchased from Santa Cruz Biotechnology (Santa Cruz, CA, USA). The final condition for p-histone H2A.X primary antibody was 500 $\times$  dilution. The secondary antibody, Alexa Fluor<sup>®</sup>488 (Cell Signaling Technology, Beverly, MA, USA), was then added in the presence of 7AAD for 30 min incubation. Finally, the cells were analyzed by flow cytometry.

#### 4.10. 8-OHdG

After fixation, 8-OHdG-detecting antibody-FITC (Santa Cruz Biotechnology) was utilized to monitor oxidative DNA damage [33]. Finally, the cells were analyzed by flow cytometry.

#### 4.11. Statistical Analysis

JMP12 software (SAS Institute, Cary, NC, USA) was used to perform ANOVA with Tukey HSD test. JMP assigns lower-case letters to each treatment. Treatments without overlapping letters were judged to have significant results for multi-comparisons  $p < 0.05$ .

### 5. Conclusions

The anticancer effects of a *Briareum excavatum*-derived bioactive compound EXCC are rarely addressed, particularly for bladder cancer. By the examination of bladder cancer cells, we validated that EXCC is a promising antiproliferation agent for bladder cancer cells in an oxidative stress-dependent manner. Several examinations such as ROS and MitoSOX supported that EXCC exerts the mechanism of oxidative stress in bladder cancer cells. EXCC also induces another oxidative stress response, such as MMP depletion. Moreover, the cellular antioxidant GSH was downregulated by EXCC, validating the modulating ability of oxidative stress by EXCC. These oxidative stress-related changes such as ROS, MitoSOX, MMP, and GSH were reverted by NAC pretreatment, indicating that EXCC is an oxidative stress-generating anticancer agent to bladder cancer cells. EXCC-promoted oxidative stress is associated with apoptosis, extrinsic and intrinsic caspase signaling, and  $\gamma$ H2AX and 8-OHdG DNA damage reverted by NAC pretreatment. In conclusion, EXCC is firstly validated to exhibit antiproliferation against bladder cancer cells, accompanied by an oxidative stress-associated mechanism.

**Supplementary Materials:** The following are available online at <https://www.mdpi.com/article/10.3390/ph15080917/s1>, Figure S1: <sup>1</sup>H NMR of EXCC measured at 28 °C (400 MHz, Me<sub>2</sub>CO-d<sub>6</sub>), Figure S2: <sup>1</sup>H NMR of EXCC measured at 0 °C (400 MHz, Me<sub>2</sub>CO-d<sub>6</sub>), Figure S3: <sup>1</sup>H NMR of EXCC measured at −20 °C (400 MHz, Me<sub>2</sub>CO-d<sub>6</sub>), Figure S4: <sup>1</sup>H NMR of EXCC measured at −40 °C (400 MHz, Me<sub>2</sub>CO-d<sub>6</sub>), Figure S5: <sup>1</sup>H NMR of EXCC measured at −60 °C (400 MHz, Me<sub>2</sub>CO-d<sub>6</sub>), Figure S6: <sup>1</sup>H NMR of EXCC measured at −80 °C (400 MHz, Me<sub>2</sub>CO-d<sub>6</sub>), Figure S7: <sup>13</sup>C NMR of EXCC measured at −60 °C (100 MHz, Me<sub>2</sub>CO-d<sub>6</sub>). References [12,50] are cited in the supplementary materials.

**Author Contributions:** Conceptualization, J.-H.S. and H.-W.C.; Data curation, C.-W.Y.; Formal analysis, C.-W.Y.; Methodology, T.-M.C., C.-H.Y. and W.-J.W.; Supervision, J.-H.S. and H.-W.C.; Writing—original draft, C.-W.Y. and J.-H.S. and H.-W.C.; Writing—review & editing, J.-H.S. and H.-W.C. All authors have read and agreed to the published version of the manuscript.

**Funding:** This work was partly supported by funds from the Ministry of Science and Technology (MOST 108-2314-B-037-021-MY3, MOST 110-2320-B-110-001-MY2, and MOST 111-2320-B-037-015-MY3), the National Sun Yat-sen University-KMU Joint Research Project (#NSYSUKMU 111-P20), the Kaohsiung Medical University (KMU-DK(A)111008), and the Kaohsiung Medical University Research Center (KMU-TC108A04).

**Institutional Review Board Statement:** Not applicable.

**Informed Consent Statement:** Not applicable.

**Data Availability Statement:** Data is contained within the article and supplementary materials.

**Acknowledgments:** The authors thank our colleague Hans-Uwe Dahms for editing the manuscript and Fang-Rong Chang for NMR supporting.

**Conflicts of Interest:** The authors declare that there are no conflict of interest among them.

## References

1. Siegel, R.L.; Miller, K.D.; Fuchs, H.E.; Jemal, A. Cancer Statistics, 2021. *CA Cancer J. Clin.* **2021**, *71*, 7–33. [[CrossRef](#)] [[PubMed](#)]
2. Powles, T.; Bellmunt, J.; Comperat, E.; de Santis, M.; Huddart, R.; Loriot, Y.; Necchi, A.; Valderrama, B.P.; Ravaud, A.; Shariat, S.F.; et al. Bladder cancer: ESMO Clinical Practice Guideline for diagnosis, treatment and follow-up. *Ann. Oncol.* **2022**, *33*, 244–258. [[CrossRef](#)] [[PubMed](#)]
3. Chang, S.S.; Bochner, B.H.; Chou, R.; Dreicer, R.; Kamat, A.M.; Lerner, S.P.; Lotan, Y.; Meeks, J.J.; Michalski, J.M.; Morgan, T.M.; et al. Treatment of non-metastatic muscle-invasive bladder cancer: AUA/ASCO/ASTRO/SUO guideline. *J. Urol.* **2017**, *198*, 552–559. [[CrossRef](#)]
4. Harraz, A.M.; El-Shabrawy, M.; El-Nahas, A.R.; El-Kappany, H.; Osman, Y. Single versus maintenance intravesical chemotherapy for the prevention of bladder recurrence after radical nephroureterectomy for upper tract urothelial carcinoma: A randomized clinical trial. *Clin. Genitourin. Cancer* **2019**, *17*, e1108–e1115. [[CrossRef](#)] [[PubMed](#)]
5. Hamid, A.R.A.H.; Ridwan, F.R.; Parikesit, D.; Widia, F.; Mochtar, C.A.; Umbas, R. Meta-analysis of neoadjuvant chemotherapy compared to radical cystectomy alone in improving overall survival of muscle-invasive bladder cancer patients. *BMC Urol.* **2020**, *20*, 1–9. [[CrossRef](#)] [[PubMed](#)]
6. Hou, X.M.; Hai, Y.; Gu, Y.C.; Wang, C.Y.; Shao, C.L. Chemical and bioactive marine natural products of coral-derived microorganisms (2015–2017). *Curr. Med. Chem.* **2019**, *26*, 6930–6941. [[CrossRef](#)]
7. Sang, V.T.; Dat, T.T.H.; Vinh, L.B.; Cuong, L.C.V.; Oanh, P.T.T.; Ha, H.; Kim, Y.H.; Anh, H.L.T.; Yang, S.Y. Coral and coral-associated microorganisms: A prolific source of potential bioactive natural products. *Mar. Drugs* **2019**, *17*, 468. [[CrossRef](#)]
8. Alves, C.; Diederich, M. Marine natural products as anticancer agents. *Mar. Drugs* **2021**, *19*, 447. [[CrossRef](#)]
9. Khalifa, S.A.M.; Elias, N.; Farag, M.A.; Chen, L.; Saeed, A.; Hegazy, M.F.; Moustafa, M.S.; Abd El-Wahed, A.; Al-Mousawi, S.M.; Musharraf, S.G.; et al. Marine natural products: A source of novel anticancer drugs. *Mar. Drugs* **2019**, *17*, 491. [[CrossRef](#)]
10. Islam, M.T.; Hossain, R.; Hassan, S.M.H.; Salehi, B.; Martins, N.; Sharifi-Rad, J.; Amarowicz, R. Biological activities of sinularin: A literature-based review. *Cell. Mol. Biol.* **2020**, *66*, 33–36. [[CrossRef](#)]
11. Wali, A.F.; Majid, S.; Rasool, S.; Shehada, S.B.; Abdulkareem, S.K.; Firdous, A.; Beigh, S.; Shakeel, S.; Mushtaq, S.; Akbar, I.; et al. Natural products against cancer: Review on phytochemicals from marine sources in preventing cancer. *Saudi Pharm. J.* **2019**, *27*, 767–777. [[CrossRef](#)] [[PubMed](#)]
12. Sheu, J.H.; Sung, P.J.; Cheng, M.C.; Liu, H.Y.; Fang, L.S.; Duh, C.Y.; Chiang, M.Y. Novel cytotoxic diterpenes, excavatolides A-E, isolated from the Formosan gorgonian *Briareum excavatum*. *J. Nat. Prod.* **1998**, *61*, 602–608. [[CrossRef](#)] [[PubMed](#)]
13. Yeh, T.-T.; Wang, S.-K.; Dai, C.-F.; Duh, C.-Y. Briacavatolides A–C, new briaranes from the Taiwanese octocoral *Briareum excavatum*. *Mar. Drugs* **2012**, *10*, 1019–1026. [[CrossRef](#)] [[PubMed](#)]
14. Chen, N.F.; Su, Y.D.; Hwang, T.L.; Liao, Z.J.; Tsui, K.H.; Wen, Z.H.; Wu, Y.C.; Sung, P.J. Briarenols C-E, new polyoxygenated briaranes from the octocoral *Briareum excavatum*. *Molecules* **2017**, *22*, 475. [[CrossRef](#)]
15. Sung, P.J.; Li, G.Y.; Su, Y.D.; Lin, M.R.; Chang, Y.C.; Kung, T.H.; Lin, C.S.; Chen, Y.H.; Su, J.H.; Lu, M.C.; et al. Excavatoids O and P, new 12-hydroxybriaranes from the octocoral *Briareum excavatum*. *Mar. Drugs* **2010**, *8*, 2639–2646. [[CrossRef](#)]
16. Sung, P.J.; Lin, M.R.; Chiang, M.Y.; Hwang, T.L. Briarexcatins V-Z, discovery of new briaranes from a cultured octocoral *Briareum excavatum*. *Bull. Chem. Soc. Jpn.* **2009**, *82*, 987–996. [[CrossRef](#)]
17. Huynh, T.H.; Chang, Y.M.; Yang, S.N.; Lee, G.H.; Wen, Z.H.; Wu, Y.J.; Su, T.R.; Sung, P.J. Briarenol L, a new chlorine-containing briarane from *Briareum excavatum* (Briareidae). *J. Mol. Struct.* **2021**, *1223*, 128970. [[CrossRef](#)]
18. Chi, W.C.; Kuo, L.M.; Yang, S.N.; Lee, Y.T.; Wen, Z.H.; Tsui, K.H.; Hwang, T.L.; Zhang, Y.L.; Sung, P.J. Briarenols O and P: Novel briaranes from a cultured octocoral *Briareum excavatum* (Briareidae). *Phytochem. Lett.* **2021**, *41*, 134–138. [[CrossRef](#)]
19. Ortega, M.J.; Zubia, E.; Sanchez, M.C.; Carballo, J.L. Cembrane diterpenes from the gorgonian *Leptogorgia laxa*. *J. Nat. Prod.* **2008**, *71*, 1637–1639. [[CrossRef](#)]

20. Marrero, J.; Benitez, J.; Rodriguez, A.D.; Zhao, H.; Raptis, R.G. Bipinnatins K-Q, minor cembrane-type diterpenes from the West Indian Gorgonian *Pseudopterogorgia kallos*: Isolation, structure assignment, and evaluation of biological activities. *J. Nat. Prod.* **2008**, *71*, 381–389. [[CrossRef](#)]
21. Velmurugan, B.K.; Yang, H.H.; Sung, P.J.; Weng, C.F. Excavatolide B inhibits nonsmall cell lung cancer proliferation by altering peroxisome proliferator activated receptor gamma expression and PTEN/AKT/NF-Kbeta expression. *Environ. Toxicol.* **2017**, *32*, 290–301. [[CrossRef](#)] [[PubMed](#)]
22. Van Engeland, M.; Nieland, L.J.; Ramaekers, F.C.; Schutte, B.; Reutelingsperger, C.P. Annexin V-affinity assay: A review on an apoptosis detection system based on phosphatidylserine exposure. *Cytometry* **1998**, *31*, 1–9. [[CrossRef](#)]
23. Boice, A.; Bouchier-Hayes, L. Targeting apoptotic caspases in cancer. *Biochim. Biophys. Acta Mol. Cell Res.* **2020**, *1867*, 118688. [[CrossRef](#)]
24. Kauffman, M.E.; Kauffman, M.K.; Traore, K.; Zhu, H.; Trush, M.A.; Jia, Z.; Li, Y.R. MitoSOX-based flow cytometry for detecting mitochondrial ROS. *React. Oxyg. Species* **2016**, *2*, 361–370. [[CrossRef](#)] [[PubMed](#)]
25. Maharjan, S.; Oku, M.; Tsuda, M.; Hoseki, J.; Sakai, Y. Mitochondrial impairment triggers cytosolic oxidative stress and cell death following proteasome inhibition. *Sci. Rep.* **2014**, *4*, 5896. [[CrossRef](#)] [[PubMed](#)]
26. Kim, S.H.; Kim, H. Inhibitory effect of astaxanthin on oxidative stress-induced mitochondrial dysfunction—A mini-review. *Nutrients* **2018**, *10*, 1137. [[CrossRef](#)]
27. Yoon, C.Y.; Lee, J.S.; Kim, B.S.; Jeong, S.J.; Hong, S.K.; Byun, S.S.; Lee, S.E. Sunitinib malate synergistically potentiates anti-tumor effect of gemcitabine in human bladder cancer cells. *Korean J. Urol.* **2011**, *52*, 55–63. [[CrossRef](#)]
28. Powles, T.; Perry, J.; Shamash, J.; Liu, W.; Oliver, T.; Joel, S. A comparison of the platinum analogues in bladder cancer cell lines. *Urol. Int.* **2007**, *79*, 67–72. [[CrossRef](#)]
29. Aldossary, S.A. Review on pharmacology of cisplatin: Clinical use, toxicity and mechanism of resistance of cisplatin. *Biomed. Pharmacol. J.* **2019**, *12*, 7–15. [[CrossRef](#)]
30. Teppo, H.R.; Soini, Y.; Karihtala, P. Reactive oxygen species-mediated mechanisms of action of targeted cancer therapy. *Oxid. Med. Cell. Longev.* **2017**, *2017*, 1485283. [[CrossRef](#)]
31. Tang, J.Y.; Ou-Yang, F.; Hou, M.F.; Huang, H.W.; Wang, H.R.; Li, K.T.; Fayyaz, S.; Shu, C.W.; Chang, H.W. Oxidative stress-modulating drugs have preferential anticancer effects-involving the regulation of apoptosis, DNA damage, endoplasmic reticulum stress, autophagy, metabolism, and migration. *Semin. Cancer Biol.* **2019**, *58*, 109–117. [[CrossRef](#)] [[PubMed](#)]
32. Wang, J.; Sun, D.; Huang, L.; Wang, S.; Jin, Y. Targeting reactive oxygen species capacity of tumor cells with repurposed drug as an anticancer therapy. *Oxid. Med. Cell. Longev.* **2021**, *2021*, 8532940. [[CrossRef](#)] [[PubMed](#)]
33. Shiau, J.P.; Chuang, Y.T.; Yang, K.H.; Chang, F.R.; Sheu, J.H.; Hou, M.F.; Jeng, J.H.; Tang, J.Y.; Chang, H.W. Brown algae-derived fucoidan exerts oxidative stress-dependent antiproliferation on oral cancer cells. *Antioxidants* **2022**, *11*, 841. [[CrossRef](#)]
34. Chen, Y.C.; Yang, C.W.; Chan, T.F.; Farooqi, A.A.; Chang, H.S.; Yen, C.H.; Huang, M.Y.; Chang, H.W. Cryptocaryone promotes ROS-dependent antiproliferation and apoptosis in ovarian cancer cells. *Cells* **2022**, *11*, 641. [[CrossRef](#)] [[PubMed](#)]
35. Sies, H. Oxidative stress: Eustress and distress in redox homeostasis. In *Stress: Physiology, Biochemistry, and Pathology*; Elsevier: Amsterdam, The Netherlands, 2019; pp. 153–163.
36. Ahmad, T.; Suzuki, Y.J. Juglone in oxidative stress and cell signaling. *Antioxidants* **2019**, *8*, 91. [[CrossRef](#)]
37. Jasek-Gajda, E.; Jurkowska, H.; Jasinska, M.; Lis, G.J. Targeting the MAPK/ERK and PI3K/AKT signaling pathways affects NRF2, Trx and GSH antioxidant systems in leukemia cells. *Antioxidants* **2020**, *9*, 633. [[CrossRef](#)]
38. Rostila, A.M.; Anttila, S.L.; Lalowski, M.M.; Vuopala, K.S.; Toljamo, T.I.; Lindstrom, I.; Baumann, M.H.; Puustinen, A.M. Reactive oxygen species-regulating proteins peroxiredoxin 2 and thioredoxin, and glyceraldehyde-3-phosphate dehydrogenase are differentially abundant in induced sputum from smokers with lung cancer or asbestos exposure. *Eur. J. Cancer Prev.* **2020**, *29*, 238–247. [[CrossRef](#)]
39. Redza-Dutordoir, M.; Averill-Bates, D.A. Activation of apoptosis signalling pathways by reactive oxygen species. *Biochim. Biophys. Acta* **2016**, *1863*, 2977–2992. [[CrossRef](#)]
40. Hung, J.H.; Chen, C.Y.; Omar, H.A.; Huang, K.Y.; Tsao, C.C.; Chiu, C.C.; Chen, Y.L.; Chen, P.H.; Teng, Y.N. Reactive oxygen species mediate Terbufos-induced apoptosis in mouse testicular cell lines via the modulation of cell cycle and pro-apoptotic proteins. *Environ. Toxicol.* **2016**, *31*, 1888–1898. [[CrossRef](#)]
41. Huang, C.H.; Yeh, J.M.; Chan, W.H. Hazardous impacts of silver nanoparticles on mouse oocyte maturation and fertilization and fetal development through induction of apoptotic processes. *Environ. Toxicol.* **2018**, *33*, 1039–1049. [[CrossRef](#)]
42. Wang, T.S.; Lin, C.P.; Chen, Y.P.; Chao, M.R.; Li, C.C.; Liu, K.L. CYP450-mediated mitochondrial ROS production involved in arecoline N-oxide-induced oxidative damage in liver cell lines. *Environ. Toxicol.* **2018**, *33*, 1029–1038. [[CrossRef](#)] [[PubMed](#)]
43. Vignon, C.; Debeissat, C.; Georget, M.T.; Bouscary, D.; Gyan, E.; Rosset, P.; Herault, O. Flow cytometric quantification of all phases of the cell cycle and apoptosis in a two-color fluorescence plot. *PLoS ONE* **2013**, *8*, e68425. [[CrossRef](#)] [[PubMed](#)]
44. Fan, H.C.; Hsieh, Y.C.; Li, L.H.; Chang, C.C.; Janouskova, K.; Ramani, M.V.; Subbaraju, G.V.; Cheng, K.T.; Chang, C.C. Dehydroxyhispolon methyl ether, a hispolon derivative, inhibits WNT/beta-catenin signaling to elicit human colorectal carcinoma cell apoptosis. *Int. J. Mol. Sci.* **2020**, *21*, 8839. [[CrossRef](#)] [[PubMed](#)]
45. Lee, C.H.; Shih, Y.L.; Lee, M.H.; Au, M.K.; Chen, Y.L.; Lu, H.F.; Chung, J.G. Bufalin induces apoptosis of human osteosarcoma U-2 OS cells through endoplasmic reticulum stress, caspase- and mitochondria-dependent signaling pathways. *Molecules* **2017**, *22*, 437. [[CrossRef](#)] [[PubMed](#)]

46. Chou, W.H.; Liu, K.L.; Shih, Y.L.; Chuang, Y.Y.; Chou, J.; Lu, H.F.; Jair, H.W.; Lee, M.Z.; Au, M.K.; Chung, J.G. Ouabain induces apoptotic cell death through caspase- and mitochondria-dependent pathways in human osteosarcoma U-2 OS cells. *Anticancer Res.* **2018**, *38*, 169–178.
47. Liu, Y.C.; Peng, B.R.; Hsu, K.C.; El-Shazly, M.; Shih, S.P.; Lin, T.E.; Kuo, F.W.; Chou, Y.C.; Lin, H.Y.; Lu, M.C. 13-Acetoxyarsocrossolide exhibits cytotoxic activity against oral cancer cells through the interruption of the Keap1/Nrf2/p62/SQSTM1 pathway: The need to move beyond classical concepts. *Mar. Drugs* **2020**, *18*, 382. [[CrossRef](#)]
48. Sgarbi, G.; Gorini, G.; Liuzzi, F.; Solaini, G.; Baracca, A. Hypoxia and IF(1) expression promote ROS decrease in cancer cells. *Cells* **2018**, *7*, 64. [[CrossRef](#)]
49. Yeh, C.C.; Tseng, C.N.; Yang, J.I.; Huang, H.W.; Fang, Y.; Tang, J.Y.; Chang, F.R.; Chang, H.W. Antiproliferation and induction of apoptosis in Ca9-22 oral cancer cells by ethanolic extract of *Gracilaria tenuistipitata*. *Molecules* **2012**, *17*, 10916–10927. [[CrossRef](#)]
50. Sung, P.J.; Lin, M.R.; Su, Y.D.; Chiang, M.Y.; Hu, W.P.; Su, J.H.; Cheng, M.C.; Hwang, T.L.; Sheu, J.H. New briaranes from the octocorals *Briareum excavatum* (Briareidae) and *Junceella fragilis* (Ellisellidae). *Tetrahedron* **2008**, *64*, 2596–2604.